PERGAMON

Aerosol Science 33 (2002) 1609–1621

Journal of
Aerosol Science

www.elsevier.com/locate/jaerosci

Parametric studies on the formation of diesel particulate matter via nucleation and coagulation modes

Donghee Kim[a,b], Mridul Gautam[a], Dinesh Gera[c,*]

[a] *Department of Mechanical and Aerospace Engineering, West Virginia University, Morgantown, WV 26506, USA*
[b] *REM Engineering Services, 3537, Collins Ferry Road, Morgantown, WV 26505, USA*
[c] *Fluent Inc., 3647 Collins Ferry Road, Morgantown, WV 26505, USA*

Received 27 May 2002; received in revised form 30 July 2002; accepted 1 August 2002

Abstract

The objective of this study is to develop a physical model that accurately accounts for the nucleation, coagulation, and condensation processes in the formation of particulate matter (PM) inside the exhaust plume of the diesel-fueled vehicles. The PM concentration has been predicted based on the fuel sulfur content, fuel-to-air ratio, exhaust flow rate, and the ambient conditions. It was predicted that the critical nucleus diameter of the particles decreased by approximately 30% and the number concentration increased by a factor of 6 with the increase in relative humidity from 10% to 90% for a fuel with 50 ppm sulfur content. The parametric studies suggested that the condensation effects are very important near the stack. Ignoring the contribution from condensation term decreased PM count median diameter from 52 to 10 nm. A fair agreement is observed between the numerically predicted PM size distribution and concentration and the experimentally measured values.

Keywords: Nucleation; Coagulation; Condensation; Plume; Diesel particulate matter

1. Introduction

In recent years, automobile industries have met stringent particulate matter (PM) emission standards primarily through advances in engine and control technologies (Kirchstetter, Harley, Kreisberg, Stolzenburgh, & Hering, 1999). Particulate matter emissions, based on mass concentrations, have

* Corresponding author. Tel.: +1-304-598-7934; fax: +1-304-598-7185.
E-mail address: dfg@fluent.com (D. Gera).

0021-8502/02/$ - see front matter
PII: S0021-8502(02)00119-2

been reduced due to improvements in the fuel injection system, control of fuel injection rate, and electronic control for precise timing of fuel injection (Sawyer et al., 1998). This is due to the fact that current emissions and air quality standards are based on the assumption that mass concentration is the critical indicator, but this assumption is no longer definitive. An example of the inadequacy of current technological advancements is that, even as the levels of total particulate mass concentrations are decreasing, the total number concentration levels of fine particulates remain unchanged or increase. Recent technical solutions aimed at reductions in total particle emissions do not necessarily result in concomitant reductions in ultra fine particle (< 100 nm) emissions; in some cases, in fact the opposite effect is observed, resulting in increased emissions of fine particles (Brown, Calyton, Harris, & King, 2000). An example of this is demonstrated by the fact that the reduction of the total mass emissions of motor vehicles in the US was by a factor of about 10, but at the same time the number of fine particles emitted increased by a factor of about 20 (Sawyer & Johnson, 1995). In recent years, the aspect of particle size that is attracting the greatest attention is the influence of fine and ultra fine particles' number concentration on human health (Kim, 2002). The knowledge of particle number concentration, which is strongly influenced by particulate matter formation during dilution of exhaust gases with the ambient air, however is very limited. The objective of this paper is to present the effect of local dilution of the diesel engine's exhaust with the ambient, relative humidity of the ambient, and the SO_2 concentration of diesel on the formation of nuclei particles, and growth of these ultra fine particles via coagulation process.

This study is important because a significant proportion of diesel emission particulates have aerodynamic diameters smaller than 1 μm. Small airborne particles less than 1 μm in diameter have a high probability of deposition in the respiratory tract, and are likely to trigger or exacerbate respiratory diseases. Small particles have also higher burdens of toxins, which when absorbed in the body can result in health consequences other than respiratory health effects (Dockery et al., 1993; Pope et al., 1995). These particles are primarily elemental carbon, but contain also adsorbed or condensed hydrocarbons, hydrocarbon derivatives, sulfur compounds, and other materials. Solvent extractable organic components of diesel aerosols represent 5–40% of the particle mass depending on the fuel and the operating conditions, e.g., engine speed, power, torque, and temperature of the vehicle (Morawska, Bofinger, Kocis, & Nwankwoala, 1998).

It is well known for some time that diesel exhaust contains large quantities of small nano-particles (Kittelson, Dolan, & Verrant, 1978), which are formed in part due to the continuation of in-stack coagulation and adsorption, along with the condensation of significant quantities of organics and inorganics present in diesel exhaust. Sulfur, found in the diesel fuels, is oxidized in the combustion chamber to give sulfur dioxide vapors, and as the exhaust gases cool in the ambient condenses to form H_2SO_4 droplets or nuclei particles (Baumgard & Johnson, 1996; Bessagnet & Rosset, 2001). The driving force for this gas-to-particle conversion process is the saturation ratio (S). For materials like the constituents of the soluble organic fraction (SOF) or sulfuric acid, the maximum saturation is achieved during dilution and cooling of the exhaust (Kittelson, 1998). The relative rates of nucleation are an extremely nonlinear function of saturation ratio (Kim, 2002; Baumgard & Johnson, 1996). From a recent comparison of an old technology and new technology engine (Kittelson, 1998), it was seen that the old technology engines take up supersaturated vapor quickly and prevent saturation ratio from rising high enough to produce nucleation, but emitted a lot of unburned carbon or soot. On the other hand, in modern low emission engines there is little surface area available to adsorb supersaturated vapors making nucleation more likely to

occur. These observations were primarily qualitative, and were used to evaluate the effect of these small particles on the environment. However, the current state-of-the-art models allow computational fluid dynamics (CFD) analysts to predict the size and concentration of these small nanosized particles.

Condensation is similar to the nucleation process, which occurs when the saturation ratio is greater than unity, except in condensation—material condenses onto the surface of the existing particles instead of forming new particles (Hinds, 1982). Ahlvik, Ntxiachristos, Keskinen, and Virtanen (1998) reported that both condensation and nucleation are dependent upon dilution ratio. It was found that lower dilution ratios lead to an increase in the saturation pressure itself, because of the respective increase in the dilution temperature.

Lushnikov and Kulmala (2000) analyzed the source-enhanced formation of disperse particles. It was inferred that the nucleation-generated particles grew as a result of the condensation and coagulation of a low volatile vapor on the particles' surfaces. Their results showed that the vapor and newly formed particles concentrations decreased with time after a short nucleation burst. Particle formation and growth was influenced by the ratio of vapor mass converted to newly formed particles and the source productivity.

It should be mentioned here that the combustion-generated particles are typically agglomerates of primary particles or "spherules" that have diameters of around 15–40 nm (Steiner, Burtscher, & Gross, 1992). The agglomeration takes place due to the relative movement and coagulation of the spherules, resulting in the formation of small clusters. Coagulation is induced by the Brownian motion of particles and also due to fluid turbulence along with various inter-particle forces. Theoretical studies have shown, however, that over the size range of the current study (20–1000 nm), neither the inter-particle forces nor turbulence are very effective (Seinfeld & Pandis, 1997). Kerminen et al. (1997) in fact, concluded that the dominating mechanism producing agglomerates in diesel exhaust is likely to be the particle Brownian movement.

There are numerous mathematical models available in the literature examining the dynamics of a wide range of particulate matter, for example, J-space transformations (Tsang & Brock, 1983), asymptotic representation (Pilinis & Seinfeld, 1987), moment methods (Williams & Loyalka, 1991; McGraw, 1997), Monte Carlo probabilistic collision algorithm (Kruis, Maisels, & Fissan, 2000; Maisels, Kruis, & Fissan, 1999; Lee & Hong, 1998), and parameterized representation (Whitby, 1981), among others. However there are a very limited number of studies available in the literature, if any, which take into account the detailed structure of the plume. The current study takes into account the detailed structure of the plume, formed by emission of exhaust gases coming out of a diesel power truck, and it is described in the next section.

2. Governing equations

An accurate and useful plume dispersion model must include the effects of turbulent mixing, convection, diffusion, temperature variations, and species transport among others. To this end, the governing transport equations for the mean fluid motion, species, and enthalpy are solved inside the wind-tunnel space using the commercial computational fluid dynamics package FLUENT^{TM} (for details, see Kim, 2002; Kim, Gautam, & Gera, 2001).

3. Discrete particle dynamics

The evolution of the particle size distribution due to coagulation, nucleation and coagulation is represented by the following discrete dynamical equation (Seinfeld & Pandis, 1997):

$$\frac{\partial C_k}{\partial t} = \underbrace{\frac{1}{2}\sum_{j=1}^{k-1}\beta_{k-j,j}C_{k-j}C_j - C_k\sum_{j=1}^{\infty}\beta_{k,j}C_j}_{\text{Coagulation}} + \underbrace{J(t)\delta(k)}_{\text{Nucleation}} + \underbrace{\beta_{1,k-1}C_1C_{k-1} - \beta_{1,k}C_1C_k}_{\text{Condensation}}, \tag{1}$$

where C_k is time (t)-dependent number concentration (No cm^{-3}) of particles of volume v_k (cm^3), β is the coagulation kernel (cm^3 No^{-1} s^{-1}) of two colliding particles, J(t) is the nucleation rate and δ is the Kronecker's delta with the value equal to 1 for the kth bin of volume v_k; and 0 otherwise. The first term on the right-hand side of Eq. (1) indicates that a particle of volume v_k can only come into existence if two particles with volumes v_j and v_{k-j} collide. The one-half is required so that each combination is counted only once.

In the present simulation, to present Brownian coagulation, the Fuchs form of the coagulation kernel $\beta_{i,j}$ is used; and it is expressed in terms of the two particle diameter D_{p1} and D_{p2} as (Fuchs, 1964)

$$\beta_{12} = 2\pi(D_1 + D_2)(D_{p1} + D_{p2})\left(\frac{D_{p1} + D_{p2}}{D_{p1} + D_{p2} + 2(g_1^2 + g_2^2)^{1/2}} + \frac{8(D_{p1} + D_{p2})}{(\bar{c}_1^2 + \bar{c}_2^2)^{1/2}(D_{p1} + D_{p2})}\right)^{-1}, \tag{2}$$

where

$$Kn_i = \frac{2\lambda_{\text{air}}}{D_{pi}},$$

$$\bar{c}_i = \left(\frac{8kT}{\pi m_i}\right)^{1/2},$$

$$l_i = \frac{8D_i}{\pi\bar{c}_i}, \tag{3a}$$

$$g_i = \frac{1}{3D_{pi}l_i}[(D_{pi} + l_i)^3 - (D_{pi}^2 + l_i^2)^{3/2}] - D_{pi}$$

and

$$D_i = \frac{kT}{3\pi\mu_t D_{pi}}\left(\frac{5 + 4Kn_i + 6Kn_i^2 + 18Kn_i^3}{5 - Kn_i + (8 + \pi)Kn_i^2}\right), \tag{3b}$$

where D_1 and D_2 are the individual Brownian diffusion coefficients, D_{p1} and D_{p2} are the diameter of each particle, Kn_i is the Knudsen number, λ is the mean-free-path of suspending gas, k is the Boltzman constant, T is the temperature, m is the mass of particle, and μ_t is the turbulent viscosity coefficient. There are various coagulation kernels available elsewhere in the literature (Tambour & Seinfeld, 1980), which are evaluated and reported elsewhere (Kim, 2002).

The H_2SO_4 hydrate (embryo) formation rate is predicted by the following nucleation equation (Kulmala, Laaksonene, & Pirjola, 1998):

$$J = C\exp(-\Delta G^*/kT), \tag{4}$$

where C is the frequency factor, k is Boltzmann's constant, T is the temperature and ΔG^* is the minimum free energy required to form an embryo. The hydration correction for the acid activities used in this research used the model suggested by Shi and Harrison (1999). Additional details on the nucleation model may be viewed elsewhere (Kim, 2002; Kim, Gautam, & Gera, 2002).

The equations arising from the various submodels described in this section are discretized using the semi-implicit finite difference scheme. Applying the volume fractions of intermediate particles, the general formula for volume-conserving equation for particle concentration can be written as (Kim et al., 2002; Jacobson, Turco, Jensen, & Toon, 1994)

$$v_k C_k^{t+1} = \left(\frac{v_k C_k^t + \Delta t \sum_{j=1}^{k} \left\{ \sum_{i=1}^{k-1} f_{i,j,k} \beta_{i,j} v_i C_i^{t+1} C_j^t \right\} + \Delta t J v_k(t)\delta(k) + \Delta t v_k \beta_{1,k-1} C_1^{t+1} C_{k-1}^{t+1}}{1 + \Delta t \sum_{j=1}^{N_B} (1 - f_{i,j,k}) \beta_{k,j} C_j^t + \Delta t \beta_{1,k-1} C_1^t} \right). \tag{5}$$

The effect of local mixing is determined by the turbulent kinetic energy of the flow and the transfer of that energy from the large-scale turbulent structures down the cascading process. The number concentration rate is affected because the partial pressure is inversely proportional to dilution ratio. Thus, the effect occurs through the saturation ratio. This effect is incorporated by dividing the right-hand side of Eq. (4) with the local dilution ratio at any given spatial location, that is (Kim, 2002)

$$v_k C_k^{t+1} = \left(\frac{v_k C_k^t + \Delta t \sum_{j=1}^{k} \left\{ \sum_{i=1}^{k-1} f_{i,j,k} \beta_{i,j} v_i C_i^{t+1} C_j^t \right\} + \Delta t v_k J(t)\delta(k) + \Delta t v_k \beta_{1,k-1} C_1^{t+1} C_{k-1}^{t+1}}{1 + \Delta t \sum_{j=1}^{N_B} (1 - f_{i,j,k}) \beta_{k,j} C_j^t + \Delta t \beta_{1,k-1} C_1^t} \right) \times \frac{1}{\text{Dilution Ratio}}. \tag{6}$$

The above equation is solved to predict the concentration variation of particulate matter in the exhaust plume of a diesel truck operating at highway speeds. In the following section, the results are compared with the measured values of particle concentrations in a wind tunnel. It is also worth mentioning that the coagulation process, manifested in the form of the beta kernel, is governed by the rate of diffusion of particles to the surface of each particle. The process is enhanced when small particles with their high diffusion coefficients diffuse to a large particle with its large surface. A 10-fold difference in particle size produces a three-fold increase in coagulation, and a 100-fold difference results in a more than 25-fold increase in coagulation rate (Willeke & Baron, 1992).

The equations arising from the various submodels described in this section are discretized using the semi-implicit finite difference scheme. The numerical prediction of particulate matter size distribution and concentration using the above sub-models is presented and discussed in the next section.

4. Simulation conditions

In recent years, considerable attention has been focused on the physical and chemical characteristics of PM emissions from internal combustion engines. It is imperative that the exhaust plume structure, and its response to the local flow and temperature fields be known under representative speed and load conditions to accurately predict the PM size and concentration from the diesel powered heavy duty vehicles. The time and spatial scales associated with the gas-to-particle transformations and particle growth are small, hence a near-field plume study becomes important. To this end, an Eulerian advection–diffusion equation with the k–ε turbulence closure (for details see Kim et al., 2001) is solved using a commercially available CFD software Fluent^{TM}, to accurately predict the plume structure from an exhaust of a diesel engine truck inside the wind tunnel.

The geometry of the heavy-duty on-road tractor truck powered by a diesel engine rated at 330 hp, which was used during a NASA Langley wind tunnel has been discretized using approximately 500,000 hexahedral and tetrahedral control volumes (cells) as shown in Fig. 1. The dimensions of the truck were 28 ft (8.4 m) long, 8 ft (2.44 m) wide and 13 ft (4 m) high, and the dimensions of the wind-tunnel test section used in the current simulation were 90 ft (27.4 m) × 60 ft (18.3 m) × 30 ft (9.1 m). The air velocity provided by fans in the wind tunnel was approximately 24.6 m/s, which simulated the situation of a truck traveling at 55 mph on a highway. The exhaust was emitted out at 29.8 m/s through a 5″ (0.13 m) diameter stack behind the truck's cabin (more detailed discussion of the experimental conditions may be found in Boyce, Mehta, Gautam, & Clark, 2000; Gautam, Xu, Ayala, & Mehta, 2000). The CO_2 concentration in the raw exhaust (undiluted exhaust) was 6% under the steady state operation of 55 mph. The gas flow in the above configuration is described by the time-averaged equations of global mass, momentum, enthalpy and species mass fractions. The standard k–ε turbulence closure and finite rate chemistry/eddy dissipation has been used in the current CFD simulation.

5. Results and discussion

To test the model, simulation results were compared to measurements of relative CO_2 concentration, temperature variations, and dilution ratios inside a dispersing plume emanating from the truck's exhaust pipe inside the Langley wind tunnel. These variations were averaged concentration and temperature values obtained at a predetermined sampling rate and time. Data were collected at the several locations perpendicular to the direction of flow inside the plume, and at certain distances downstream of the source along the centerline of the plume. The dilution ratio (DR), an important parameter for the current simulation, was measured from the ratio of the raw CO_2 concentration (C_0) to the value of CO_2 at a given location $C(x, y, z)$ as

$$\mathrm{DR} = \frac{C_0 - \text{Background Concentration}}{C(x, y, z) - \text{Background Concentration}}. \tag{7}$$

The DR predicted from the CFD model is compared with the experimental data measured along the centerline of the plume elsewhere (Kim et al., 2001). The curve fit for the dilution ratio as a

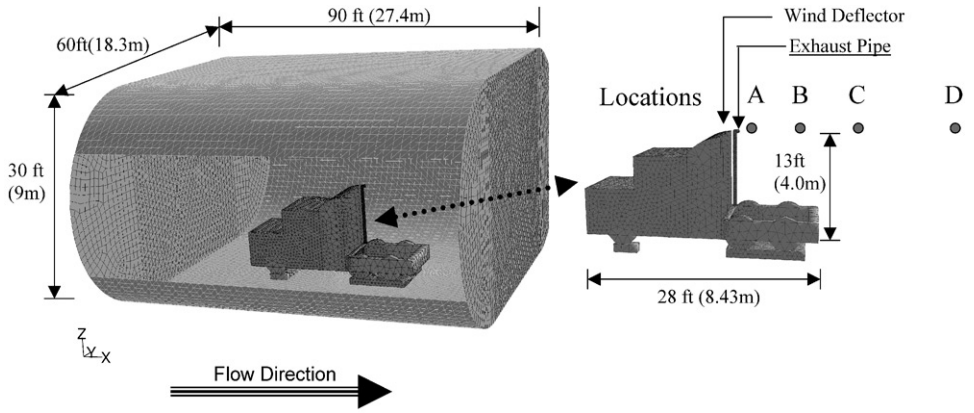

Fig. 1. Computational grid of truck inside the wind tunnel. (Locations A, B, C and D are 20″ (0.5 m), 80″ (2.0 m), 200″ (5.0 m), and 337″ (8.6 m), respectively, from the source.)

function of the distance (x), measured in meters is found to be of the form (Kim, 2002)

$$\mathrm{DR} = 16.1x^{1.36}. \tag{8}$$

In order to determine the nucleation rate, it is necessary to convert the fuel sulfur to the H_2SO_4 vapor pressure in dilution tunnel as done previously by Baumgard and Johnson (1996). First, the exhaust SO_4 concentration can be determined from the following relation:

$$[\mathrm{SO_4}] = (F/A)(\%\ \text{fuel sulfur})(\%S\ \text{to}\ \mathrm{SO_4}\ \text{conv.})(M_{\mathrm{SO4}}/M_{\mathrm{exhaust}})(1 - F/A)\ \text{density}), \tag{9}$$

where $(F/A = 0.035)$ is the fuel-to-air ratio, $M_{\mathrm{SO_4}}$ is the molecular weight of SO_4, M_{exhaust} is the apparent molecular weight of the exhaust stream, $\%S$ to SO_4 is assumed to be 0.04 (Baumgard & Johnson, 1996; Shi & Harrison, 1999), and the density of air is assumed to be 1.186 kg/m^3. The next step is to convert the actual dilution tunnel SO_4 concentration to H_2SO_4 vapor pressure. Noting that m/V is the H_2SO_4 concentration, the vapor pressure $P_{\mathrm{H_2SO_4}}$ can be determined by using the ideal gas equation:

$$P_{\mathrm{H_2SO_4}} = (m/V)RT/M, \tag{10}$$

where V is the volume (m^3), R is the universe gas constant, M is the molecular weight of exhaust, and T is the temperature.

The PM size distribution and concentration obtained from Eq. (6) with the contribution from nucleation, coagulation and condensation terms at location A (20″ from the stack outlet; see Fig. 1 for location) is shown in Fig. 2. The PM size distribution at location A is presented at 200 ms. The elapse of 200 ms is calculated by assuming that location A is approximately 5 m from the exhaust valves of the diesel engine where the nucleation process is first initiated, and the exhaust is coming out at the rate of 25 m/s. In the present case, geometric ratios of 1.4, 1.2, and 1.05 were tried to check the grid-independent solutions. It was found that there was no significant difference in the results obtained from the geometric ratio of 1.2 and 1.05. Hence, the geometric ratio of 1.05 is used for the discretization of bin sizes in the current computations. It may also be seen from Fig. 2 that if the contribution from condensation term is included then the PM count median diameter (CMD: inferred from the peak diameter) shifts to the right from approximately 10–52 nm. This

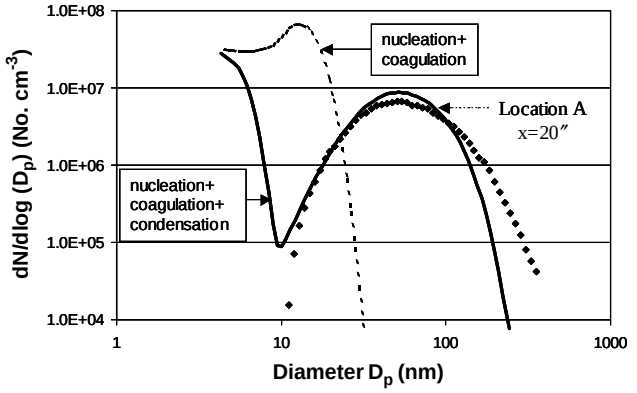

Fig. 2. Particle concentration variation with diameter at a location 0.5 m (20″) from the stack outlet by considering (a) nucleation+coagulation, and (b) nucleation+coagulation+condensation effects; (—) numerical model; (♦) experimental data.

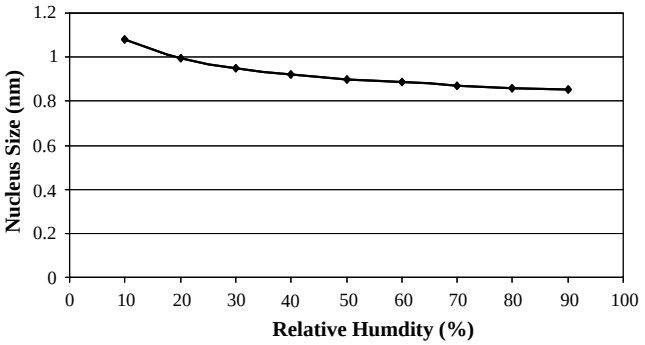

Fig. 3. Effect of critical nucleation diameter as a function of relative humidity.

shift may be attributed to the fact that the condensation essentially increases the nucleus radius. A slight asymmetry in the curve around CMD may be attributed to the difference in the rate of production of new particles by nucleation and the rate of coagulation of these particles to form bigger particles from the existing particles via collisions. In the beginning, nucleation rate is high and the coagulation rate is small. As the time progresses the nucleation rate does not change significantly but the nucleus size increases, consequently, the coagulation/agglomeration process is enhanced because these nuclei particles with their high diffusion coefficients diffuse to large particles with large surface area. The collision of small particles with large particles increases the particle size but reduces the total number of particles at any given instant, and causes the CMD to skew to its right. It is worth mentioning that near the stack outlet, where the rapid dilution of PM concentration with the ambient air is taking place, condensation effects are very important. Additionally, the dip near 10 nm in Fig. 2 indicate that the nucleation mode (typically less than 10 nm) is dominant, and the coagulation/agglomeration of particles is causing the particle diameter to increase.

The effect of relative humidity on critical nucleation particle diameter (stable diameter) at temperature 25°C is shown in Fig. 3. Higher the relative humidity, smaller the particle diameter is

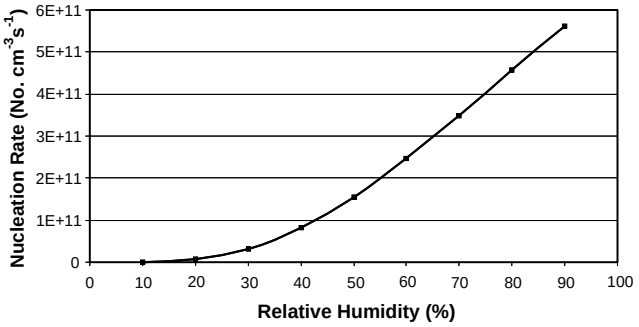

Fig. 4. Effect of relative humidity on nucleation rate at 25°C.

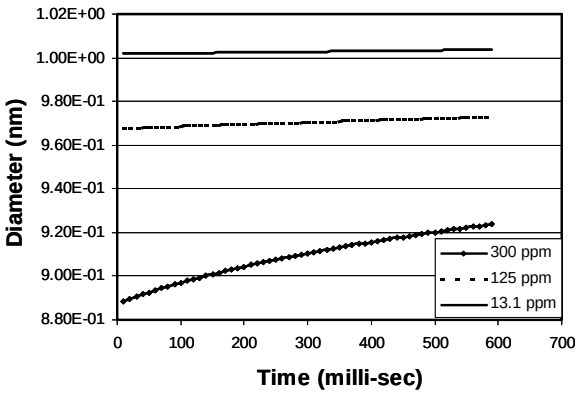

Fig. 5. Effect of fuel sulfur content on nucleus diameter with time for 35% relative humidity.

necessary to become a stable particle. At the lower relative humidity, it requires more energy to get over the saddle point and, therefore, more molecules are necessary to obtain this energy and consequently the particle diameter is large.

The effect of relative humidity on nucleation rate at temperature 25°C is shown in Fig. 4. The trend indicates that the higher relative humidity enhances nucleation. At the higher relative humidity, the bulk phase density of the water molecules also increases, leading to more molecules colliding pre unit time. Therefore, nucleation rate increases with the increasing relative humidity.

Fig. 5 shows the temporal variation of nucleus diameter with time in fuels with different fuel sulfur content at a constant relative humidity 35%. As the sulfur fuel content increases, the nucleus diameter also decreases. The nucleus diameter increases more rapidly with time at sulfur fuel content 300 ppm compared with the sulfur fuel content of 125 ppm or 13.1 ppm.

These current computations have been tested for different fuel sulfur level. The effects of different sulfur level (13.1 and 125 ppm) on particle diameter and concentration for the constant relative humidity (30%) are shown in Figs. 6 and 7, respectively. It may be seen that the model predictions agree well qualitatively with the experimentally measured values at 0.14 and 0.17 s. The part of the discrepancy in the comparison of particle number concentration from the numerical model may be

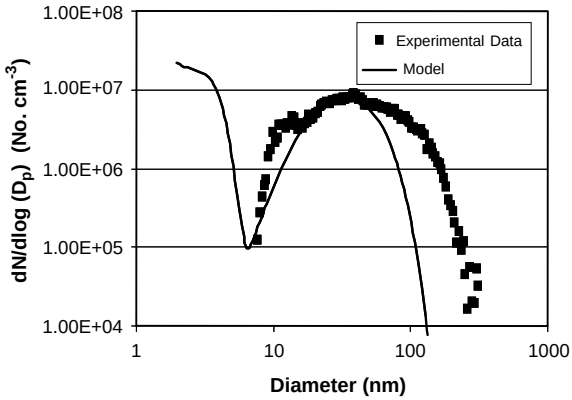

Fig. 6. Comparison with experimental data of particle concentration variation with diameter (sulfur fuel level = 13.1 ppm, relative humidity = 30%, dilution ratio = 10).

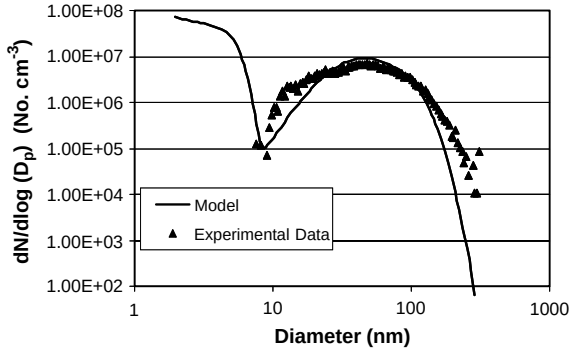

Fig. 7. Comparison with experimental data of particle concentration variation with diameter (sulfur fuel level = 125 ppm, relative humidity = 30%, dilution ratio = 5).

due to the fact that the interaction of volatile organic compounds, ash in lubricating oil, and the unburned carbon from the fuel droplets is not considered in the present numerical models. Also, volatile organic species are not considered here, though there is evidence that for low sulfur fuel they are dominant. Additionally, in low sulfur fuels the precursor to nucleation may actually be the simultaneous presence of NO_x and SO_x, which may transform to HNO_3 and H_2SO_4 vapors, respectively. Both of these gases have affinity to saturate water vapors.

Fig. 8 presents the effect of different sulfur fuel content (13.1 and 125 ppm) on particle diameter and concentration at 0.14 and 0.34 s, respectively. It is worth mentioning that the count median diameter (CMD) for fuel with sulfur content of 125 ppm shifted to the right more quickly than fuel with sulfur content of 13.1 ppm. This may be due to the fact that higher fuel–sulfur concentration results in higher SO_4 concentration in the exhaust. As particles grow, the H_2SO_4 particle molar fraction decreases due to the addition of H_2O molecules, and the vapor pressure above the particles surface decreases. When the particle's H_2SO_4 or H_2O vapor pressure equals the species atmospheric vapor pressure, the number of molecules striking the particles surface equals the number of molecules

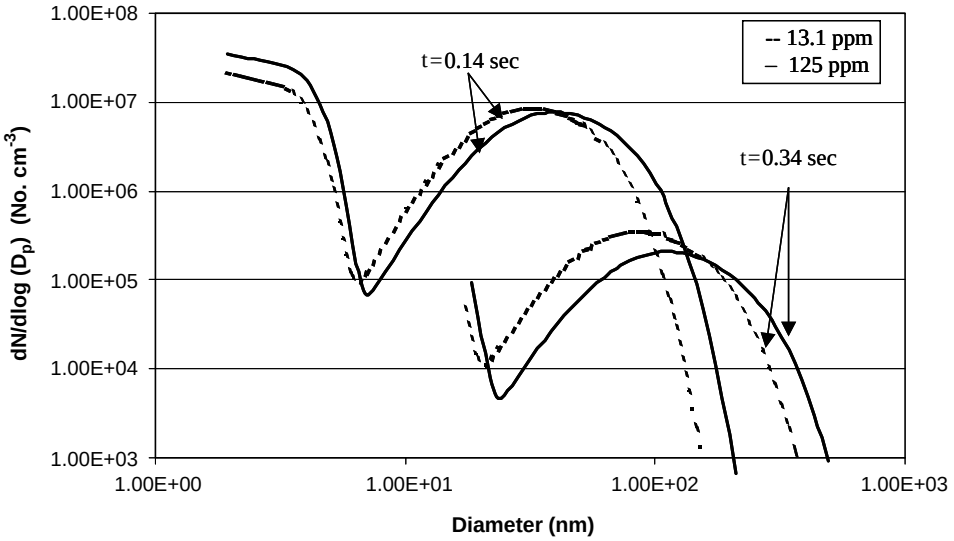

Fig. 8. Particulate matter prediction on different sulfur fuel level (13.1 and 125 ppm) at 0.14 and 0.34 s.

leaving the surface, and the particle diameter will become stable. Also, a bigger critical diameter of particles will result in much faster growth of the particles because of coagulation.

6. Conclusions

The nucleation rates in the formation of PM were calculated directly from the sulfur content in the fuel, and hydration effects were included in the nucleation sub-model. It was inferred from the current parametric studies that the critical nucleus diameter decreased by approximately 30% and the number concentration increased by a factor of 6 with the increase in relative humidity from 10% to 90% for a fuel with 50 ppm sulfur content. The similar trends were also predicted for the fuels with 13.1, 125, and 300 ppm sulfur content. It was inferred that the condensation effects were very important near the stack outlet where the rapid dilution of particulate matter with the ambient air was dominant. It was predicted that if the contribution from the condensation term was included then the PM count median diameter increased from approximately 10–52 nm. A good agreement was seen between the predicted PM concentration values and the PM concentrations measured at four different locations in a turbulent plume from the diesel exhaust in the wind tunnel.

References

Ahlvik, P., Ntxiachristos, L., Keskinen, J., & Virtanen, A. (1998). *Real time measurements of diesel particle size distribution with an electrical low pressure impactor*. SAE 980410.

Baumgard, K. J., & Johnson, J. H. (1996). *The effect of fuel and engine design on diesel exhaust particle size distributions.* SAE 960131, Society of Automobile Engineers (pp. 37–50).

Bessagnet, B., & Rosset, R. (2001). Fractal modeling of carbonaceous aerosols—application to car exhaust plumes. *Atmospheric Environment*, *35*, 4751–4762.

Boyce, J., Mehta, S., Gautam, M., & Clark, N. N. (2000). Heavy duty diesel truck research in the ODU/Langley wind tunnel (CRC E-43). *10th CRC on-road vehicle emissions workshop*, San Diego, CA, March 27–29, 2000.

Brown, J. E., Calyton, M. J., Harris, D. B., & King Jr., F. G. (2000). Comparison of the particle size distribution of heavy-duty diesel exhaust using a dilution tailpipe sampler and an in-plume sampler during on-road operation. *Journal of Air & Waste Management Association*, *50*, 1407–1416.

Dockery, D. W., Pope, C. A., Xu, X., Spengler, J. D., Ware, J. H., Fay, M. E., Ferris, B. G., & Seizer, F. E. (1993). An association between air pollution and mortality in six U.S. cities. *Massachusetts Medical Society Journal of Medicine*, *329*, 1753–1759.

Fuchs, N. (1964). *The mechanics of aerosols*. New York: The Macmillan Company.

Gautam, M., Xu, Z., Ayala, A., & Mehta, S. (2000). Diesel exhaust plume studies. Wind tunnel experiments and modeling. *Fourth ETH nanoparticle measurement workshop*, Zurich, August 7–9, 2000.

Hinds, W. (1982). *Aerosol technology-properties, behavior, and measurement of airborne particles*. New York: Wiley.

Jacobson, M. Z., Turco, R. P., Jensen, E. J., & Toon, O. B. (1994). Modeling coagulation among particles of different composition and size. *Atmospheric Environment*, *28*, 1327–1338.

Kerminen, V.-M., Mkel, T. E., Ojanen, C. H., Hillamo, R. E., Vilhunen, J. K., Rantanen, L., Havers, N., Bohlen, A. V., & Klockow, D. (1997). Characterization of the particulate phase in the exhaust from a diesel car. *Environmental Science and Technology*, *31*, 1883–1889.

Kim, D. (2002). *Nucleation and coagulation modes in the formation of particulate matter inside the exhaust of a diesel vehicle*. Ph.D. dissertation, West Virginia University, Morgantown, WV. [Electronically available from the following web site: http://etd.wvu.edu/templates/showETD.cfm?recnum=2305.]

Kim, D., Gautam, M., & Gera, D. (2001). On the prediction of concentration variations in a dispersing heavy-duty truck exhaust plume using k–ε turbulent closure. *Atmospheric Environment*, *35*, 5267–5275.

Kim, D., Gautam, M., & Gera, D. (2002). Modeling nucleation and coagulation modes in the formation of particulate matter inside a turbulent exhaust plume of a diesel engine. *Journal of Colloid and Interface Science*, *249*, 96–103.

Kittelson, D. B. (1998). Engines and nanoparticles: A review. *Journal of Aerosol Science*, *29*, 575–588.

Kittelson, D. B., Dolan, D. E., & Verrant, J. A. (1978). *Investigation of a diesel exhaust aerosol*. Society of Automobile Engineers, SAE 780109.

Kirchstetter, T. W., Harley, R. A., Kreisberg, N. M., Stolzenburgh, M. R., & Hering, S. V. (1999). On-road measurement of fine particle and nitrogen oxide emissions from light- and heavy-duty motor vehicles. *Atmospheric Environment*, *33*, 2955–2968.

Kruis, F. E., Maisels, A., & Fissan, H. (2000). Direct simulation Monte-Carlo method for particle coagulation and aggregation. *A.I.Ch.E. Journal*, *46*, 1735–1742.

Kulmala, M., Laaksonene, A., & Pirjola, L. (1998). Parameterizations for sulfuric acid/water nucleation rates. *Journal of Geophysical Research*, *103*, 8301–8307.

Lee, J. W., & Hong, B. H. (1998). Monte Carlo studies on three-species two-particle diffusion-limited reactions. *Physica A*, *256*, 351–358.

Lushnikov, A. A., & Kulmala, M. (2000). Foreign aerosol in nucleating vapor. *Journal of Aerosol Science*, *31*, 651–672.

Maisels, A., Kruis, F. E., & Fissan, H. (1999). Direct Monte Carlo simulations of coagulation and aggregation. *Journal of Aerosol Science*, *30*, S417–S418.

McGraw, R. (1997). Description of aerosol dynamics by the quadrature method of moments. *Aerosol Science and Technology*, *27*, 255–265.

Morawska, L., Bofinger, N. D., Kocis, L., & Nwankwoala, A. (1998). Submicrometer and supermicrometer particles from diesel vehicle emissions. *Environmental Science and Technology*, *32*, 2033–2042.

Pilinis, C., & Seinfeld, J. H. (1987). Continued development of a general equilibrium model for inorganic multicomponent atmospheric aerosols. *Atmospheric Environment*, *21*, 2453–2466.

Pope, C. A., Thun, M. J., Namboodriri, M. M., Dockery, D. W., Evans, J. S., Speizer, F. E., & Heath, C. W. (1995). Particulate air pollution as a predictor of mortality in a prospective study of U.S. adults. *American Journal of Respiratory Critical Care Medicine*, *151*, 669–674.

Sawyer, R. F., Harley, R. A., Cadle, S. H., Norbeck, J. M., Slott, R., & Bravo, H. A. (1998). *Mobile sources critical review*. 1998 NARSTO Assessment, Report to Coordinating Research Council, Atlanta, GA.

Sawyer, R. F., & Johnson, J. H. (1995). *Diesel emissions and control technology*, *chapter in diesel exhaust*: *A critical analysis of emissions*, *exposure and heath effects*. A Special Report of the Institute's Diesel Working Group, Health Effects Institute (pp. 65–81).

Seinfeld, J. H., & Pandis, S. N. (1997). *Atmospheric chemistry and physics*: *From air pollution to climate change*. New York: Wiley.

Shi, J. P., & Harrison, R. M. (1999). Investigation of ultrafine particle formation during diesel exhaust dilution. *Environmental Science and Technology*, *33*, 3730–3736.

Steiner, D., Burtscher, H., & Gross, H. (1992). Structure and disposition of particles from a spark-ignition engine. *Atmospheric Environment*, *26A*, 997–1003.

Tambour, Y., & Seinfeld, J. H. (1980). Solution of the discrete coagulation equation. *Journal of Colloid Interface Science*, *74*, 260–272.

Tsang, T. H., & Brock, J. R. (1983). Simulation of condensation aerosol growth by condensation and evaporation. *Aerosol Science and Technology*, *2*, 311–320.

Whitby, K. T. (1981). Determination of aerosol growth rates in the atmosphere using lumped aerosol dynamics. *Journal of Aerosol Science*, *12*, 174–178.

Willeke, K., & Baron, P. A. (1992). *Aerosol measurement*: *Principles techniques and applications*. New York, NY: Van Nostrand Reinhold.

Williams, M. M. R., & Loyalka, S. K. (1991). *Aerosol science, theory and practice*. Oxford: Pergamon Press.